



UNIVERSITY OF LEEDS

This is a repository copy of *Non-assembly Walking Mechanism for Robotic In-Pipe Inspection*.

White Rose Research Online URL for this paper:

<https://eprints.whiterose.ac.uk/179085/>

Version: Accepted Version

Proceedings Paper:

Jackson-Mills, GH, Shead, BA, Collett, JR et al. (7 more authors) (2021) Non-assembly Walking Mechanism for Robotic In-Pipe Inspection. In: Lecture Notes in Networks and Systems. CLAWAR 2021, 30 Aug - 01 Sep 2021, Virtual. Springer Verlag , pp. 117-128. ISBN 9783030862930

https://doi.org/10.1007/978-3-030-86294-7_11

Reuse

Items deposited in White Rose Research Online are protected by copyright, with all rights reserved unless indicated otherwise. They may be downloaded and/or printed for private study, or other acts as permitted by national copyright laws. The publisher or other rights holders may allow further reproduction and re-use of the full text version. This is indicated by the licence information on the White Rose Research Online record for the item.

Takedown

If you consider content in White Rose Research Online to be in breach of UK law, please notify us by emailing eprints@whiterose.ac.uk including the URL of the record and the reason for the withdrawal request.



eprints@whiterose.ac.uk
<https://eprints.whiterose.ac.uk/>

Non-Assembly Walking Mechanism for Robotic In-Pipe Inspection

Dr. G.H. Jackson-Mills¹, and B.A. Shead¹, J. R. Collett¹, M. Mphake¹, Dr. N. Fry¹,
Dr. A.R. Barber¹, Dr. J.H. Boyle¹, Prof. R.C. Richardson¹, Dr. A. E. Jackson¹, S.
Whitehead¹

¹ Department of Mechanical Engineering, University of Leeds, LS2 9JT, United Kingdom
Email: g.jackson-mills@leeds.ac.uk

Abstract. The manufacture and assembly of small-scale robotics can be expensive and time-consuming using traditional methods; especially when complex mechanisms are involved. By refining current additive manufacturing techniques a micro-scale walking robot can be 3D printed without the need for any complex mechanical assembly. The robot requires only the addition of simple circuitry and 2 motors, one for each of the 1 degree of freedom walking mechanisms before it is capable of being driven wirelessly. Once fully assembled, differential drive of the parallel leg sets allows for locomotion in any direction on a 2-D plane. The robot's compact size; just 62mm (x) x 38mm (y) x 88mm (z), and leg curvature makes travel possible through borehole/pipe diameters as low as 65mm. By pushing printer tolerances to the limit, complex mechanisms can work in Non-Assembly at a small scale. Through the application of these Non-Assembly techniques to field robots such as those intended for use in the Pipebots project could allow for the production of large swarms of robots quickly and affordably.

Keywords: Robot, 3D Printing, Walking, In-Pipe.

1 Introduction

Pipebots aims to revolutionise buried pipe infrastructure management with the development of micro-robots designed to work in underground pipe networks and dangerous site. This project will include the analysis of both clean and waste water pipelines in systems that cannot readily be accessed by humans without invasive excavation procedures. Small, tight, in-pipe environments are common in aging waste water systems, such as those in Figure 1 these spaces are well suited to miniature robots. Capable of allowing human pilots remote operative access, in-pipe environments can be inspected safely using robots without invasive, expensive, and environmentally unfriendly excavation procedures. Inspection of these spaces can require different approaches; access points can often vary in size. One specific robot may be unequipped to deal with all

eventualities of the mission. For example it may be too large or have the wrong locomotion method. This type of inaccessible environment scenario can commonly be found in waste water pipelines.

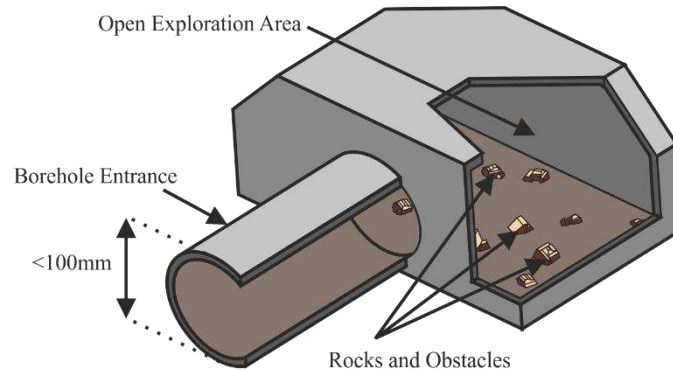


Figure 1: Inaccessible environment scenario cutaway with a 100mm borehole entrance into an open area.

Additive manufacturing (3D printing) allows rapid fabrication of functional robotic parts and has become popular due to the quick turnaround from model to physical prototype. The relative affordability and accessibility of 3D printing vs. traditional subtractive manufacturing methods, has led to the creation of many Non-Assembly mechanical designs. Non-Assembly printable designs work straight off the printing bed as intended with no fasteners, connectors or glue required.

Work has been done on the effectiveness of these techniques in respect to robotic part creation [1], and even in Non-Assembly animal models such as moveable joints in a functional 3D printed elephant [2]. These techniques have been applied to create Non-Assembly versions of historical mechanisms such as slider-crank and ratchets [3]. Even universal joints have been printed as functional Non-Assembly parts out of stainless steel [4]. Cornell University created an untethered 3D-Printed mechanical insect which utilized 3D printed wing structures [5]. Tufts University capitalized on the use of soft material printing to create a soft robot with full steering control based on the caterpillar of the tobacco hawk moth [6]. Robot hands have been fully printed with shape memory alloy actuation [7], and even origami-based methods have been employed to create Non-Assembly medical gripping arms [8]. By applying these Non-Assembly printing techniques, specially adapted robots can be created rapidly from a library of pre-made designs. If these robots could be printed fully assembled off the print bed, a new robot could be produced and deployed in a matter of hours after the addition of actuation and control systems. In a case such as Figure 1, a small (<100mm) borehole or pipe adjoins a larger open and otherwise inaccessible space which must be explored. In this environment with open sections, specialized pipe robots which rely on wall-pressing, such as those using screw, inch-worm and PIG mechanisms, become ineffective as the surrounding walls are too far away. Small agile robots are suited to overcome the obstacles likely to be found within chambers comprised of earth and deposit build up. Figure 2 introduces simplified versions of potential robotic solutions for

this case. A review of in-pipe robotics locomotion methods [9] shows A-C are capable of both in-pipe and open space exploration on a small-scale.

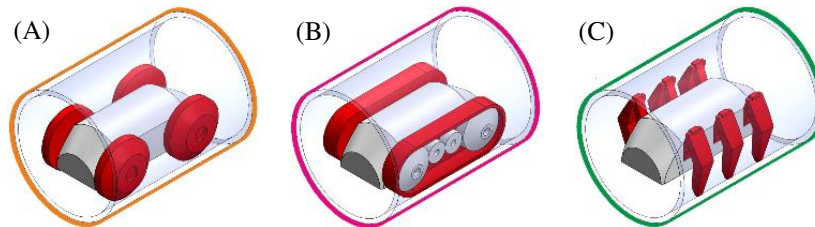


Figure 2: Potential robot locomotion solutions, (A) Wheeled, (B) Tracked (C) Walking [9]

Each solution is suitable for Non-Assembly printing, with different levels of complexity. Wheeled robots (A) are relatively simple, typically using a direct motor transmission to drive wheels. Tracked systems (B) are slightly more complex requiring a sprocket and accompanying belt to be printed in-situ. In the interest of showcasing the potential of Non-Assembly robotics the most challenging locomotion method has been chosen for development namely walking robots (C), which require an intricate linkage mechanism at this scale. These types of robot are particularly good at stepping over uneven ground such as that in Figure 1. This work will present the development of a walking robot to demonstrate Non-Assembly techniques.

2 Walking Robot Design

The walking robot is specified to be small-scale (able to fit through a 100mm borehole), quick to produce, inexpensive and simple to assemble. Small robots in this size range (50mm – 100mm length) predominantly use simple locomotion methods based on 1-2 actuators. The system will therefore utilise a two-motor drive which is the most compact choice available that still allows a differential drive steering method. This posed a challenge, as many larger walking robots are complex to control and include multiple degrees of freedom within each leg. This walking mechanism will have just one degree of freedom to be driven forwards or backwards using a single DC motor. The system will be mirrored to form one whole robot with differential steering.

2.1 Control System Design Overview

The robot's control system has been kept as simple as possible, using off-the-shelf components and only two actuators. The robot is controlled using a 3.3V version of the Arduino Pro Mini which interfaces wirelessly over serial using the SparkFun Bluetooth Mate Silver. The low-level logic voltage uses less power than the 5V version at the cost of processing speed but is still compatible with all secondary components. A SparkFun

Dual Motor Driver is used to control the direction of the two motors (and hence steering), and two 3.3V LED's act as headlights. The whole system runs on a 260mah 7.4V Lithium Polymer (LiPo) rechargeable battery which supplies regulated 3.3V to the Arduino and raw voltage to the dual motor driver board. Commands are given to the Pro Mini via serial commands sent from a master computer running LabVIEW. The circuitry required adds an estimated 30 minutes to the assembly due to the time it takes to solder. The circuit boards, LEDs and motors simply slide into the printed grooves in the body and are held in place by friction. A summary of the materials used in the production of one unit, including price and weight, can be found in Table 1.

Table 1: Bill of Materials

Part No.	Component	Quantity Req.	Weight (g)	Price (£)
1	Pololu MicroMetalGear 6V Motor	2	19.0	25.78
2	Arduino Pro Mini 328 3.3V/8MHz	1	2.00	8.00
3	SparkFun Bluetooth Mate Silver	1	12.0	20.06
4	SparkFun Dual Motor Driver	1	2.00	7.20
5	Arduino LilyPad LED	2	0.50	2.27
6	Turnigy 260mah 2S 35~70C LiPo	1	14.0	4.13
7	3D Printed Lower Chassis	1	25.0	64.00
8	3D Printed Upper Chassis	1	18.0	64.00
9	3D Printed Motor Shaft Gear	2	0.50	4.00
10	Screw M2 x 14mm	3	1.50	0.05
TOTAL		12	94.5g	£199

2.2 Walking Mechanism Design

In order to maintain the small size stipulated in the robot specifications, a hexapod design with three legs on each side was selected. Two legs per side would not provide static stability during the locomotion gait, and more than three would require a longer chassis. The mechanism is required to contain one degree of freedom per side and allow forwards or reverse actuation of each mechanism independently. The one D.O.F walking mechanism was first developed and refined to produce a desired gait. CAD software was used for creation of simplified planar mechanisms and to perform a motion study as shown in Figure 3.

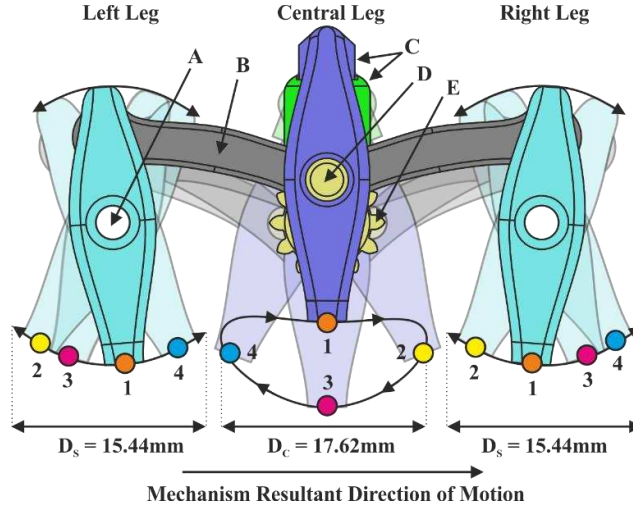


Figure 3: Walking mechanism gait design. Where the numbered and coloured circles show the positions of each leg on their respective paths at 0° (1/Orange), 90° (2/Yellow), 180° (3/Pink), 270° (4/Blue).

The linkage system for each side is driven through a single crank in the central leg (Figure 3, D), with only 1 D.O.F. the gait cycle was fully defined during the mechanism design stage. It is designed to be driven by a bevel gear pinion which would push-fit directly onto the DC motor D-shaft. Power is transmitted to the leg through an identical bevel gear (E) giving a 1:1 gear ratio. Each bevel crank (D/E) is supported at either end in ABS to ABS contact keeping it central and providing stability of the transmission mechanism. The front and back legs are driven via links (B) attached to the crank on the middle leg such that they move in a rocking motion pivoting on chassis pins (A). The prismatic slider which is paired with the central leg (C) achieves the stepping motion required by forcing linear movement of the central leg from a defined point of rotation. The walking motion produced in this linkage layout exploits the more complex 2D motion of the central leg to lift the front and back legs off the ground during their swing phases. The points of one motion cycle (1-4) displayed in Figure 3 occur at 0° (1/Orange), 90° (2/Yellow), 180° (3/Pink), 270° (4/Blue). The peak driving force of the gait occurs at point 3 where the central leg has lifted the body to its maximum height off the ground. From points 3 to 4 the rocking side legs sweep the robot forwards in sync with the central legs movement to point 4. This repeated motion drives the robot forwards a theoretical total distance as calculated using Equation 1 where the step lengths D_C , D_S , are calculated from the CAD model.

$$D_T = D_C + D_S \quad (1)$$

Where:

- $D_T =$ Total distance per revolution crank
- $D_C =$ Central leg step in x
- $D_S =$ Side leg step in x

$$D_T = 17.62 + 15.44 = 33.06\text{mm}$$

A motion analysis study of the legs was undertaken, showing the displacement of the ‘foot’ on each leg of the walking mechanism in Figure 4. Each displacement path corresponds to the numbered paths taken by the foot of each leg highlighted on the CAD model, Figure 3.

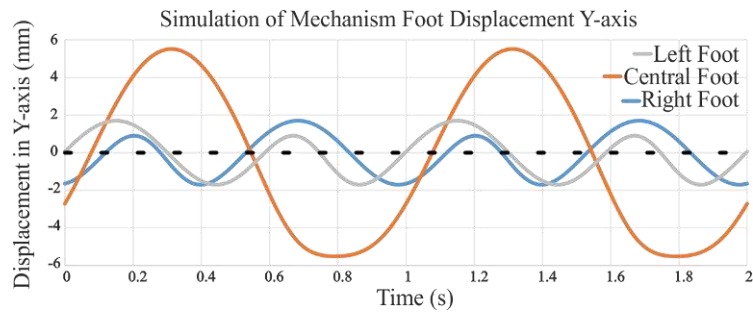


Figure 4: Simulation of mechanism foot displacement showing the displacement of the three legs in relation to each other during the mechanism drive cycle, where a negative value indicates that the foot of the leg is in driving contact with the ground.

Ideally the step heights of each leg would be equal, but the length of the robot limits the passive leg’s length. Increasing their length at this body size would cause them to clash with the central leg. The walking mechanism and electronics system was then incorporated into the design of the chassis. The chassis houses the components in Table 1 in the most compact way possible, allowing only 2mm walls between components. Modifications were made to the legs, giving them a curved profile that allows more efficient space utilisation in cylindrical access points. This essentially gives the robot a circular cross-section.

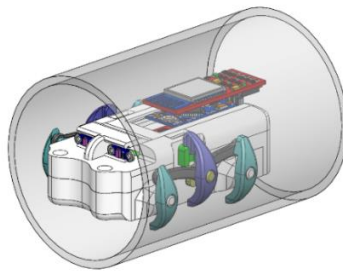


Figure 5: Assembled robot In-Pipe

The feet of each leg contain rubber pads for increased friction with the ground. These pads are manufactured along with the feet by utilizing the printer’s multi-material capabilities. By combining rigid and flexible materials within the printer, elastomers can effectively be created joined to solid sections.

3 3D Printing and Assembly

3.1 Modifications for Non-Assembly Printing

Printing the designed robot with a Non-Assembly approach requires the generation and export of a specially tailored STL file from the existing CAD model. Modifications included the addition of shaft tolerances to avoid fusing separate links in the mechanism and splitting of the chassis to facilitate integration of the control system and removal of support. The largest challenge when printing a system like this lies in optimising tolerances. The minimum gap between moving parts must be large enough to avoid fusing them and allow support removal, while also being as small as possible to reduce play in the joints. A test piece was printed to determine the correct tolerance for the printer in question (Stratasys Objet 1000). This machine can print to an accuracy of $85\mu\text{m}$ for features smaller than 50mm such as those used in this design. Using this information, a test was devised to determine the minimum clearance needed in a CAD model shaft assembly. Six 3mm diameter shafts were mated axially within six holes increasing in size from 3.0mm to 3.5mm with increments of 0.1mm. Figure 6 shows the 3D printed test piece, in which the shafts capable of moving are marked with a Y and unmovable (fused) shafts are marked with an X. The smallest hole that allowed movement was 3.2mm, so a standard clearance gap of 0.1mm was used for all moving parts in the mechanism.

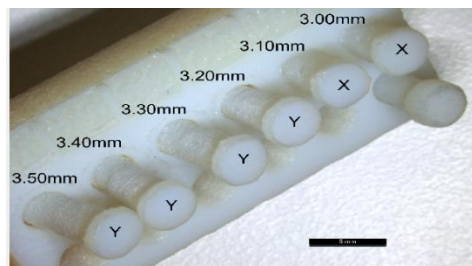


Figure 6: 3D printed shaft tolerance test (black bar = 1 mm).

In the final design, each shaft is mated concentrically with a hole of diameter of the shaft + 0.2mm. This is shown in Figure 7 (left), along with a cross section highlighting the shafts and linkages where these were applied. The robot had to be split into two parts to allow removal of internal support material and mounting of the electronics. Screws were used to attach the two halves and lock the motors and battery in place. The print assembly includes 4 parts in total; lower chassis, upper chassis, and two bevel pinions in Figure 7. The robot was printed using Objet's digital ABS material, which consists of RGD515 (60g) and RGD535 (4g). The total build time for one robot is 296 minutes.

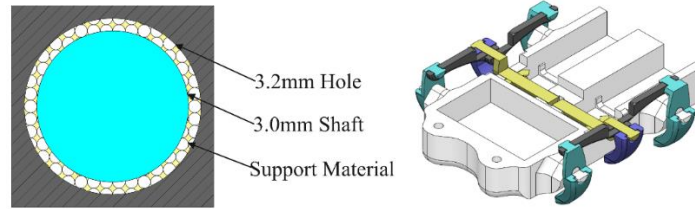


Figure 7: 3D printed mechanism shaft tolerances (left). Cross-sections of shaft print arrangement (right).

3.2 Robot Assembly

Assembly first requires the removal of support material from the finished printed parts (Figure 8). The Objet printer used SUP705 gel-like photopolymer as its support material, which is printed in any negative space to separate solid objects in the assembly. This requires half an hour of cleaning as the support is not dissolvable and requires manual removal. Once removed from the printer and cleaned, the two halves of the robot were assembled. This is a simple process and requires only the addition of the motors, circuitry and batteries. Components either slide into inbuilt grooves or are constrained by recesses in the body. The central leg (Dark Blue) is then coupled with the prismatic slider on the upper half (Green) forcing the mechanism to rotate with the correct gait. Three screws are then inserted to fasten the upper and lower chassis together. Dimensions of the Pololu micro metal motors used are 10mm x 12mm x 35mm. The inner walls of the body as shown in Figure 8 are 10mm x 12mm in order constrain the motor position and allow only movement in the Z-axis. Movement in the Z-axis is only required for assembly, after which the motors become fully constrained due to fastening of the top plate. The design incorporates tailored grooves that mate with the motor housing as well as a small wall placed to stop the motor at the bevel meshing point, thus defining position along the Z-axis.

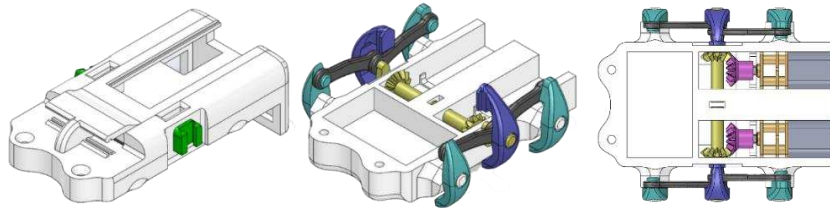


Figure 8: Upper (left) and lower chassis (centre) when printed. Top-down view with motors and pinions inserted (right).

Using an assembled walking mechanism drastically reduces the total number of pieces that need to be assembled. The walking mechanism uses 10 parts on each side of the robot for a total of 21 including the base. By printing the mechanism fully assembled, only the lower and upper chassis require assembly, effectively eliminating 20 parts before the addition of connectors.

4 Robot Performance

To test the robot's walking performance it was fully assembled, Figure 9 shows the robot with all the control electronics mounted and motors wired up. The Bluetooth radio board is placed on top for reliable signal transmission to the computer. Using the Bluetooth receiver LabVIEW sends serial commands to the robot which allows it to be teleoperated by a human pilot.

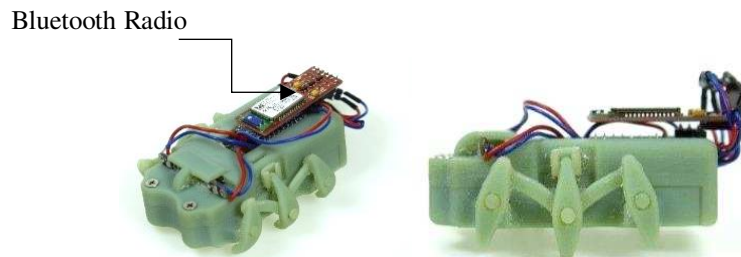


Figure 9: 3D printed walker fully assembled with electronics.

To assess the robot's precision of movement, a test was conducted in a controlled environment using an Optotrak Certus system which is an active sensor-based motion capture system with a positional accuracy of approximately $\pm 0.1\text{mm}$. The study evaluated the accuracy of the Non-Assembly printed walking mechanism when commanded to drive in a straight line. The robot was fitted with a tracker on the front of the nose and was placed directly in line with the Y-axis on the 3-axis reference hub. The robot-mounted tracker required its own power supply, necessitating a tethered connection to the data acquisition unit, limiting the distance it could travel to 300mm. Both of the robot's DC motors were then driven forwards using identical PWM signals, to theoretically achieve a straight path of motion along the Y-axis. The (X, Y) position data gathered across 16 repetitions is shown in Figure 10. The robot has a tendency to curve right, probably due to slightly different motor speeds. The robot travels between -50mm and +150mm off course within the X-axis range away from the desired path, $X = 0$. To determine the error the motors were run for 60 seconds and the number of motor revolutions compared; the left motor was found to be 15% slower than the right.

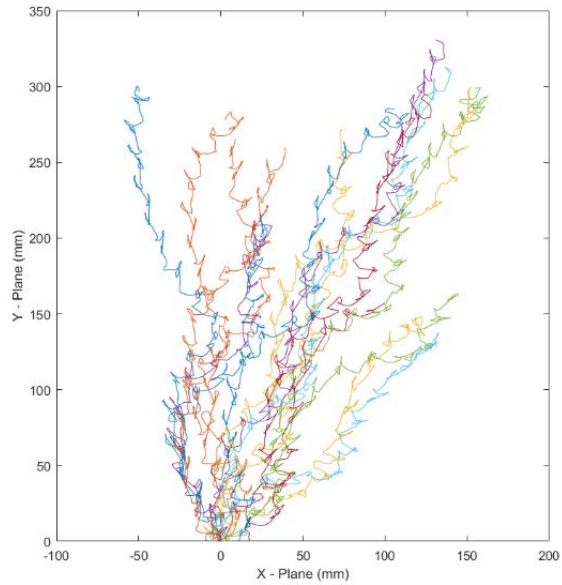


Figure 10: Robots 16 straight path trajectories over 300mm.

The tests took place over an average of 30 seconds at full speed so the right mechanism will be a full 4 repetitions ahead of the left at the end of the course. This caused the robot to veer right over a 300mm distance in most experiments. This intermittent backwards motion is an artefact of the locomotion gait (see stills in Figure 11). The robot tends to tip backwards at certain points in the gait cycle, most obviously in image 7 where the central leg is at its highest position causing the robot to tilt (the robot's centre of mass is behind the middle legs). The tracking sensor registers this pitching motion as negative displacement in the Y-axis. There is also a roll movement due to de-syncing of the left and right walking mechanisms. To keep the robot compact the DC motors have no encoders and thus no feedback on the current position of the mechanism relative to the gears. This gradual change in phase between the left and right legs causes body roll as one side mechanism of the robot reaches the lowest point in the gait as the other one reaches the highest, resulting in a difference in speed such that the left and right walking mechanisms are not in perfect anti-phase.

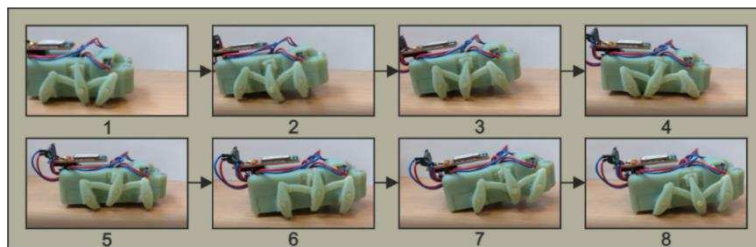


Figure 11: Video stills showing the robots walking gait.

4.1 Discussion

The walking robot design allows the manufacture of a complex walking mechanism without the need for complex assembly. By transmitting power only to the central crank to a one degree of freedom mechanism minimal assembly is required and allows the robot to move with just two simple follower legs. The main disadvantage of this central leg driven mechanism design rather than driving a front or back leg, necessitating a longer body to house the motor properly. Printing this model as-is on a printer with lower resolution than the 85 μ m of the Objet1000 should be done with caution. The tolerances of the mechanism would likely need to be increased from the current 0.1mm clearance standard. Suitable types of printers for this kind of Non-Assembly device would not only meet the accuracy requirements but also use suitable support materials. Different types of support materials can be used based on the printer type, most of which are removable from the part. Polyvinyl Alcohol (PVA) is water-soluble and can be removed through immersion in water. Selective Laser Sintering (SLS) uses the powder-based build material to support the part, and this simply falls away from the part after printing. Scaling up the Non-Assembly print would effectively reduce the effects of tolerance stacking in the robot and improve the control of the system. The 0.1mm tolerance standard currently used to avoid fusing of components (Figure 7) would remain the same but the error percentage between shaft and hole would decrease with an increase in shaft size. Figure 10 showed that the robot does not currently move in a reliably straight direction, so to fix the 15% DC motor speed errors encoders could be added to the motors.. Using a PID controller these two values can be constantly matched; however, this still leaves the position of the mechanism unknown. To achieve optimal gait patterns the control system should know the absolute position of the mechanism on each side, so they can be matched and the two halves can be run in sync.

The robot does require minimal assembly having been split in two halves, this is not necessary for the mechanism itself. Rather, the split was incorporated in the design to facilitate installation, removal and replacement of components such as motors by sliding into the motor slots. This was useful during testing of the prototype but in a finalized product this would be done with a pick and place machine. A final version would also see a decrease in production price. Table 1 states the bill of materials required to assemble the robot. The price is quoted as £199 to produce one unit, but the printing costs for the chassis account for 66% of this price. This price is based on the production of one robot, charged at a £26 hourly rate for use of the Objet 1000 printer and a printing time of 5 hours. Cost per robot could be reduced if the robot were to be printed in batches. By applying the principles of Non-Assembly Printing this robot is proof of concept for small complex robotic systems.

5 Conclusion

The development of this system has proven that small complex mechanisms can be 3D printed using “Non-Assembly” techniques. By pushing printer tolerances to the limit and developing a one degree of freedom walking mechanism that can be driven from a single motor, the robot could be 3D printed and assembled in just 2 pieces. The removal of intricate assembly methods greatly reduces the time required to build the robot. The system is small-scale and can fit through a pipe, borehole, or gap of 65mm or greater making it well suited to exploration in tight situations. The price of the prototype system is estimated at just £200, 66% of which comes from printing costs. Reduced production labour makes these robots quick to produce and send on exploration missions in a “fire and forget” manner that aligns with the Pipebots projects in-pipe robotic swarm theme. The robot does not represent a major investment and hence retrieval in a field deployment is of low priority. Future work on this design will likely be focused on refining locomotion methods for dealing with non-standard in-pipe geometries, and reducing cleaning time from support material remains.

References

1. De Laurentis Kathryn, J. "Rapid Fabrication of Non-Assembly Robotic Systems with Embedded Components." *Robotics and Mechatronics Laboratory*: 1-30.
2. Cali, Jacques, et al. "3D-printing of non-assembly, articulated models." *ACM Transactions on Graphics (TOG)* 31.6 (2012): 130.
3. Lipson, Hod, et al. "3-D printing the history of mechanisms." *Journal of Mechanical Design* 127.5 (2005): 1029-1033.
4. Yang, Yong-qiang, et al. "Rapid fabrication of metallic mechanism joints by selective laser melting." *Proceedings of the Institution of Mechanical Engineers, Part B: Journal of Engineering Manufacture* 225.12 (2011): 2249-2256.
5. Richter, Charles, and Hod Lipson. "Untethered hovering flapping flight of a 3D-printed mechanical insect." *Artificial life* 17.2 (2011): 73-86.
6. Umedachi, Takuya, and Barry A. Trimmer. "Design of a 3D-printed soft robot with posture and steering control." *Robotics and Automation (ICRA), 2014 IEEE International Conference on*. IEEE, 2014.
7. De Laurentis, Kathryn J., and Constantinos Mavroidis. "Rapid fabrication of a non-assembly robotic hand with embedded components." *Assembly Automation* 24.4 (2004): 394-405.
8. Mehta, Ankur M., and Daniela Rus. "An end-to-end system for designing mechanical structures for print-and-fold robots." *Robotics and Automation (ICRA), 2014 IEEE International Conference on*. IEEE, 2014.
9. Mills, G. H., Jackson, A. E., & Richardson, R. C. (2017). Advances in the inspection of unpiggable pipelines. *Robotics*, 6(4), 36.